Structural and functional models for [NiFe] hydrogenase

Angamuthu, R.

6

Hexanuclear (Ni_6-)Metallacrown as Functional Model for [NiFe] Hydrogenase†

Abstract. The hexanuclear $[Ni_6(cpss)_{12}]$ (cpss = μ–S–CH_2–CH_2–S–C_6H_4–Cl) wheel-type cluster adopts an unusual structural motif whereby four NiS_4 square-planar and two NiS_5 square-pyramidal units are conjoined by edge sharing; the NiS_5 units resemble the inactive state of the Ni centre in [NiFe] hydrogenase. In addition, the hexanuclear metallacrown has been demonstrated to functionally resemble the [NiFe] hydrogenases. Protonation of the cluster was studied employing ^{1}H NMR spectroscopy by the sequential additions of dichloroacetic acid or *p*-toluenesulfonic acid monohydrate into solutions of $[Ni_6(cpss)_{12}]$ in CD_2Cl_2 and DMF-d_7, respectively; protonation takes place on the thioether sulfurs available in the metallacrown. Electrochemical properties of both the parent and protonated $[Ni_6(cpss)_{12}]$ species have been studied using cyclic voltammetry. Protonated $[Ni_6(cpss)_{12}]$ shows an interesting electrocatalytic property, as it catalyses the reduction of protons into molecular hydrogen in the presence of protic acids, such as dichloroacetic acid and chloroacetic acid at –1.5 and –1.6 V *vs*. Ag/AgCl in DMF, respectively. A catalytic cycle has been proposed based on the observations from the NMR spectroscopic and electrochemical studies of the metallacrown. The behavior of this electrocatalyst was further studied by its immobilization on the surface of a edge plane pyrolytic graphite electrode; reduction of a dichloroacetic acid solution in acetonitrile on the surface of the modified electrode occurs at 220 mV more positive potential compared to the unmodified electrode.

---

† This chapter is based on: R. Angamuthu, H. Kooijman, M. Lutz, A. L. Spek and E. Bouwman, *Dalton Trans.*, **2007**, 4641-4643; R. Angamuthu and E. Bouwman, *Phys. Chem. Chem. Phys.*, **2009**, 5578-5583.

6.1. Introduction

Metal thiolates, including nickel thiolates, are of interest in the context of their rich redox chemistry[1,2] and structural diversity in supramolecular architectures;[3] moreover, as synthetic models for environmentally and industrially significant enzymes like hydrogenases.[4-6] Despite the fact that there are plenty of examples for the ubiquitous O- and/or N-bridged metallacrowns,[7-15] few literature reports are available concerning S-bridged supramolecules.[16-19] Cyclic structures $[(Ni(\mu\text{-}SR)_2)_n]$ (n = 4-11) with a range of monodentate thiolates and bidentate (NS,[17,18] S_2[16]) thiolates are known since the first report[19] of a hexanuclear wheel. Noticeably all these reported cyclic structures are composed of square-planar NiS_4 units as building blocks. Interestingly, an example of a decanuclear cluster crystallized with an encapsulated benzene molecule as a guest has recently been reported.[3]

On the other hand, growing concerns about global warming and the threat regarding to the depletion of conventional fossil fuels induces the surge towards sustainable energy sources. Dihydrogen is generally accepted to be one of the most promising and sustainable energy alternatives for fossil fuels. Researchers are toiling in different directions to find viable ways to produce dihydrogen, effectively and economically.[20-26] One of the ways suggested by Nature is using the ideas and insights from enzymes such as hydrogenases; these efficiently reduce protons into dihydrogen.[27] Numerous structural and functional models of hydrogenases have been reported[1,2,4,28,29] in the past decade since the report of the crystal structure of a hydrogenase.[30] A number of [NiRu] complexes, based on [Ni(xbsms)][31] [H_2xbsms = *α*,*α*'-bis(4-mercapto-3,3-methyl-2-thiabutyl)-*o*-xylene] and [Ni(emi)][32] [H_2emi = 1,2-ethylenebis(2-mercaptoisobutyramide)] have been recently reported as electrocatalysts to produce dihydrogen around –1.5 V vs. Ag/AgCl in DMF, using triethylamine hydrochloride as a proton source.[23,33,34]

Some of the recently reported heterodinuclear [NiFe] model complexes are structurally similar to the active site of the [NiFe] hydrogenase. However, they are stable only at low temperatures, possibly due to the presence of multiple carbonyl ligands.[35,36] Consequently, there has been considerable interest in stable and efficient electrocatalysts, such as nickel and cobalt complexes of macrocycles and multinuclear metallacrowns, as they can be potentially employed in PEM (Proton Exchange Membrane) water electrolysis cells.[21,24,37,38] A handful of transition-metal complexes, away from the interest of modeling the active site of hydrogenases, have also been reported to reduce protons into dihydrogen effectively with various overpotentials ranging between –1.5 and –0.2 V vs. SCE.[20-26,28,29,39-41]

A series of cobalt difluoroboryl-diglyoximate complexes have been reported recently to catalyze the electrochemical dihydrogen evolution at overpotentials as low as –0.20 V vs. SCE in acetonitrile.[24,37,38,42] The dinuclear complex [$(CpMo–\mu–S)_2S_2CH_2$] has been reported as an electrocatalyst in the dihydrogen production showing almost 100% current efficiency when *p*-cyanoanilinium tetrafluoroborate was used as a proton source.[26] The oxothiomolybdenum wheel $Li_2[Mo_8S_8O_8(OH)_8(oxalate)]$ has recently been shown to be a electrocatalyst producing dihydrogen from $HClO_4$, *p*-toluenesulfonic acid, trifluoroacetic acid and acetic acid at –1 V vs. SCE.[21] However, a credible comparison of the electrocatalytic efficiency cannot be made among the reported electrocatalysts as they work in different environments and produce dihydrogen from various proton sources.

This chapter reports on the synthesis, reactivity and structural features of the first example of a hexanuclear cluster having square-planar, as well as square-pyramidal coordinated nickel ions in the same molecule. In addition, the protonation and electrocatalytic dihydrogen evolution studies of this extremely stable low-spin hexanuclear nickel thiolate metallacrown are assessed with the assistance of various techniques.

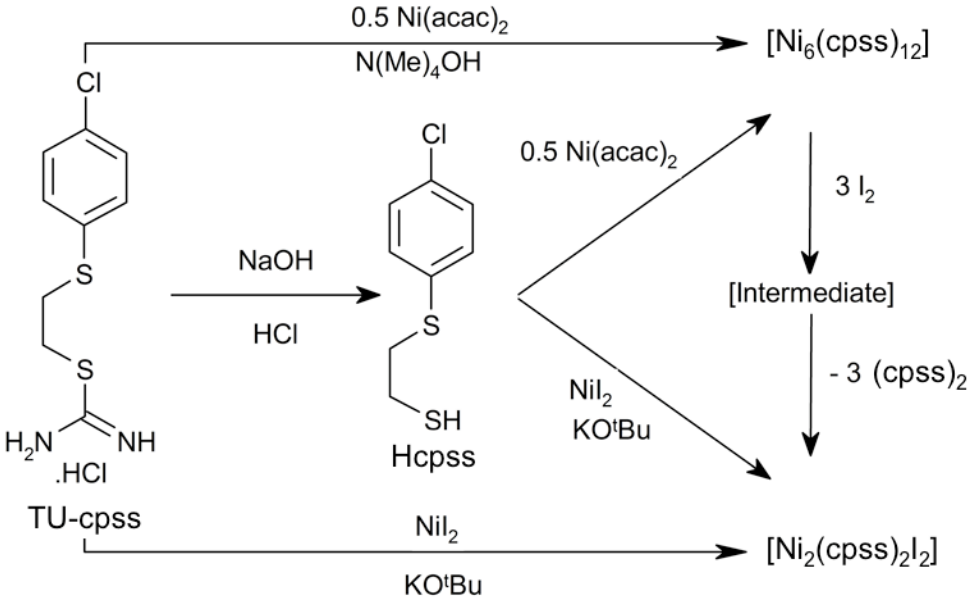

Scheme 6.1. Synthesis of complexes [$Ni_6(cpss)_{12}$] and [$Ni_2(cpss)_2I_2$] from TU-cpss, and the chemical oxidation of [$Ni_6(cpss)_{12}$] by iodine.

6.2. Results and Discussion

6.2.1. Synthesis

The reaction of $Ni(acac)_2$ with two equivalents of the thiouronium salt TU-cpss (Scheme 6.1) in the presence of two equivalents of tetramethylammonium hydroxide led

to an immediate colour change to deep brown and the thiolate-bridged hexanuclear nickel complex $[Ni_6(cpss)_{12}]$ was isolated as reddish-brown crystals. Reaction of three equivalents of iodine with one equivalent of $[Ni_6(cpss)_{12}]$ in dichloromethane resulted in a color change from dark brown to deep greenish brown. Filtration and slow evaporation of the solvent in air yielded dark brown hexagonal plates of the complex $[Ni_2(cpss)_2I_2]$ suitable for X-ray diffraction.

6.2.2. X-ray Crystal Structure Description of $[Ni_6(cpss)_{12}]$

The X-ray crystal structure determination of reddish–brown rectangular-shaped crystals revealed a hexanuclear metallacrown $[Ni_6(cpss)_{12}]$ framework (Fig. 6.1) containing four square-planar NiS_4 and two square-pyramidal NiS_5 units joined by edge sharing. The whole molecule resides on a crystallographic inversion centre. Although the ligand has been synthesized to act as a bidentate chelate, it is coordinating only via the thiolate sulfur in 10 out of the 12 ligands that are present in $[Ni_6(cpss)_{12}]$. Each nickel ion is surrounded by four thiolate sulfurs of the μ-$SCH_2CH_2SC_6H_4Cl$ ligands with Ni–S distances of 2.1895(17)–2.2161(16) Å in a distorted square-planar fashion. However, one of the four ligands coordinated to Ni(3) acts as a chelating bidentate ligand; its thioether sulfur is coordinated at the apical position making the coordination geometry of Ni(3) square-pyramidal with a τ value[43] of 0.15.

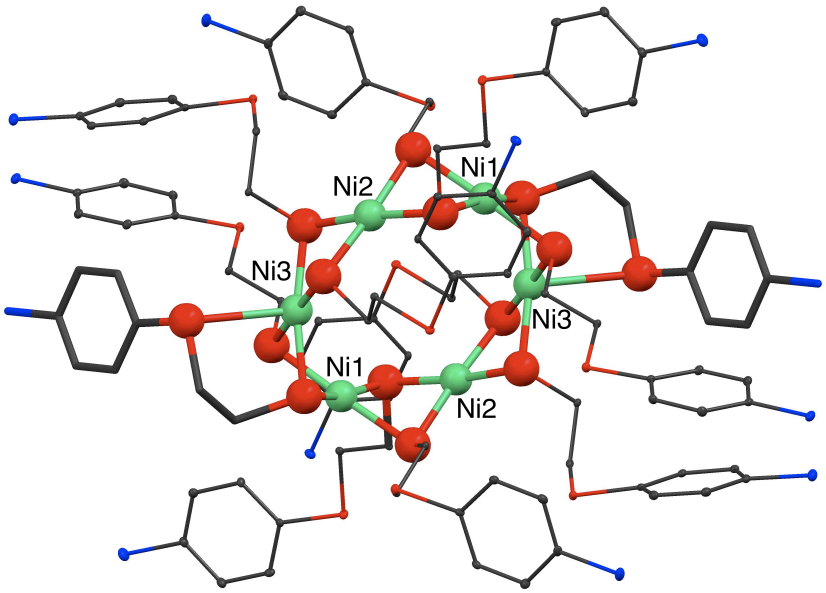

Fig. 6.1. Perspective view of $[Ni_6(cpss)_{12}]$. Ni, green; S, red; Cl, blue; C, grey. Hydrogens are omitted for clarity. Symmetry operation a: −x, 1−y, −z. Selected bond lengths (Å): Ni–S, 2.1895(17)–2.2161(16); Ni···Ni, 2.8220(11)–3.1022(12).

The two NiS_5 units resemble the Ni centre of the oxidized inactive state in the [NiFe] hydrogenase.[44] The nickel ions approximately form a hexagon, with Ni···Ni separations in the range of 2.8220(11)–3.1022(12) Å. Two μ-S bridges from two ligands connect adjacent nickel ions. The twelve μ-S atoms form double crowns, one above and the other below the Ni_6 ring. Owing to the geometrical restrictions introduced by the bridging sulfur atoms, the NiS_4 units are not strictly planar; the nickel ions Ni(1), Ni(2) and Ni(3) are 0.121, 0.026 and 0.119 Å above their corresponding S_4 planes, respectively. The S–Ni–S *cis* bond angles range from 81.88(6) to 98.31(6)°. The ellipsoidal Ni_6 ring with Ni–Ni–Ni vertex angles of 118.84(3)–129.39(4)°, has a distance range between 5.4081(12) and 6.3316(13) Å for opposite nickel ions. The Ni(2)···Ni(2) distance is noticeably shorter (5.4081(12) Å) in comparison with the Ni(1)···Ni(1) distance (6.3316(13) Å). The ligands that are coordinated to Ni(1) are involved in π–π stacking to a neighboring hexanuclear molecule with a stacking distance of 3.854(4) Å. On the other hand, the chelating ligand coordinated to the Ni(3) ion shows a comparatively weaker stacking (3.902(4) Å) while the non-chelating ligand coordinated to the same nickel ion is involved in a comparatively stronger stacking interaction (3.771(4) Å). These asymmetric π–π stacking interactions may contribute to the ellipsoidal shape of the Ni_6 hexagon and the orientation of the ligands as present in the solid-state structure.

6.2.3. Reactivity of [$Ni_6(cpss)_{12}$] with Iodine and the Structure of [$Ni_2(cpss)_2I_2$]

In order to shed light on the solution structure and to make use of the reactive axial sites of the nickel ions of complex [$Ni_6(cpss)_{12}$], its oxidation with three equivalents of iodine was performed in dichloromethane, which resulted in a color change of the dichloromethane solution from dark brown to deep greenish brown. Filtration and slow evaporation of the solvent in air yielded dark brown hexagonal plates of the complex [$Ni_2(cpss)_2I_2$] suitable for X-ray diffraction.

The ability of the ligand to coordinate via the thioether sulfur is evidenced by the formation of [$Ni_2(cpss)_2I_2$]. The X-ray crystal structure determination revealed a dinuclear structure with crystallographic twofold symmetry (Fig. 6.2), in which two ligands bridge the two Ni ions through the thiolate sulfurs, and the thioether sulfurs and iodide ions occupy the terminal positions of the nickel ions. Thus, two NiS_3I square-planar units are conjoined at an edge, and the Ni_2S_2 rhombus is folded with a dihedral angle of 66.28(2)° with an intramolecular Ni···Ni separation of 2.8602(4) Å. The Ni–S distances are quite normal in [$Ni_2(cpss)_2I_2$], the Ni–S thioether distance (2.1940(7) Å) is slightly longer than the Ni–S thiolate distances (2.1658(7) and 2.1902(7) Å). The crystal packing of [$Ni_2(cpss)_2I_2$] along the *c* axis shows a one-dimensional chain formed by the intermolecular interaction between the chlorides and the centroids of the electron-

deficient aromatic rings (C-Cl···Cg(π-ring)) at a distance of 3.696 Å.[45,46] ^{1}H and ^{13}C NMR spectra of $[Ni_2(cpss)_2I_2]$ reveal more or less the same chemical shift values, as interpreted for the chelating ligand in $[Ni_6(cpss)_{12}]$.

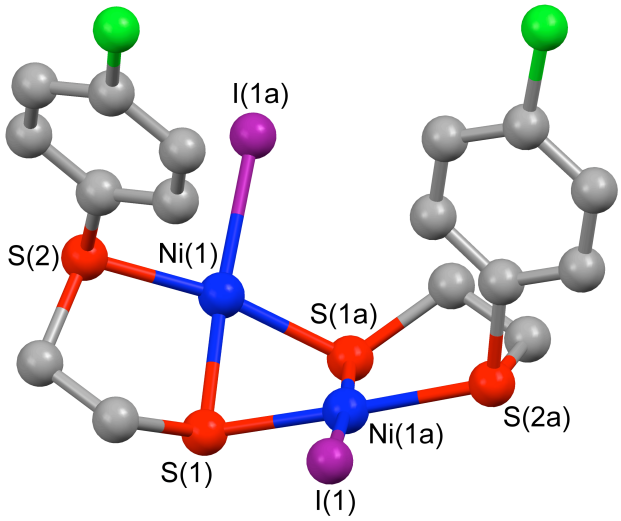

Fig. 6.2. Perspective view of $[Ni_2(cpss)_2I_2]$. Ni, blue; S, red; Cl, green; I, violet; C, grey. Hydrogens are omitted for clarity. Symmetry operation a: 1 − x, y, 0.5 − z. Selected bond lengths (A˚): Ni(1)–S(1), 2.1658(7); Ni(1a)–S(1), 2.1902(7); Ni(1)–S(2), 2.1940(7); Ni(1)···Ni()1a, 2.8602(4).

6.2.4. Electrochemical Studies of $[Ni_6(cpss)_{12}]$ and $[Ni_2(cpss)_2I_2]$

The electrochemistry of $[Ni_6(cpss)_{12}]$ in a dichloromethane solution shows only an irreversible oxidation process, observed at 0.77 V vs. Ag/AgCl (Fig. 6.3). The chemical oxidation of $[Ni_6(cpss)_{12}]$ has been achieved by adding three equivalents of iodine to a dichloromethane solution of $[Ni_6(cpss)_{12}]$ in an electrochemical cell. The CV of the unstable oxidized species has been recorded immediately. The quasi-reversible reduction of the Ni(III) species is observed at 0.60 V with reoxidation at 0.66 V. Within a few minutes, a white sediment is deposited at the bottom of the cell, which by NMR proved to be the disulfide of the ligand. The complex $[Ni_2(cpss)_2I_2]$ shows a quasi-reversible oxidation at 0.740 V, of which the reduction occurs at 0.46 V.

In addition, the cyclic voltammograms of $[Ni_6(cpss)_{12}]$ (0.5 mM) were recorded at a static glassy carbon working electrode in a DMF solution containing 0.05 M tetra-*n*-butylammonium hexafluoridophosphate in order to assess the effect of coordinating solvent. This solution displays a reductive event at –1.12 V, which is attributed to the irreversible reduction process of Ni^{II} to Ni^{I}, and an irreversible oxidation process of Ni^{II} to Ni^{III} at 0.72 V vs Ag/AgCl.

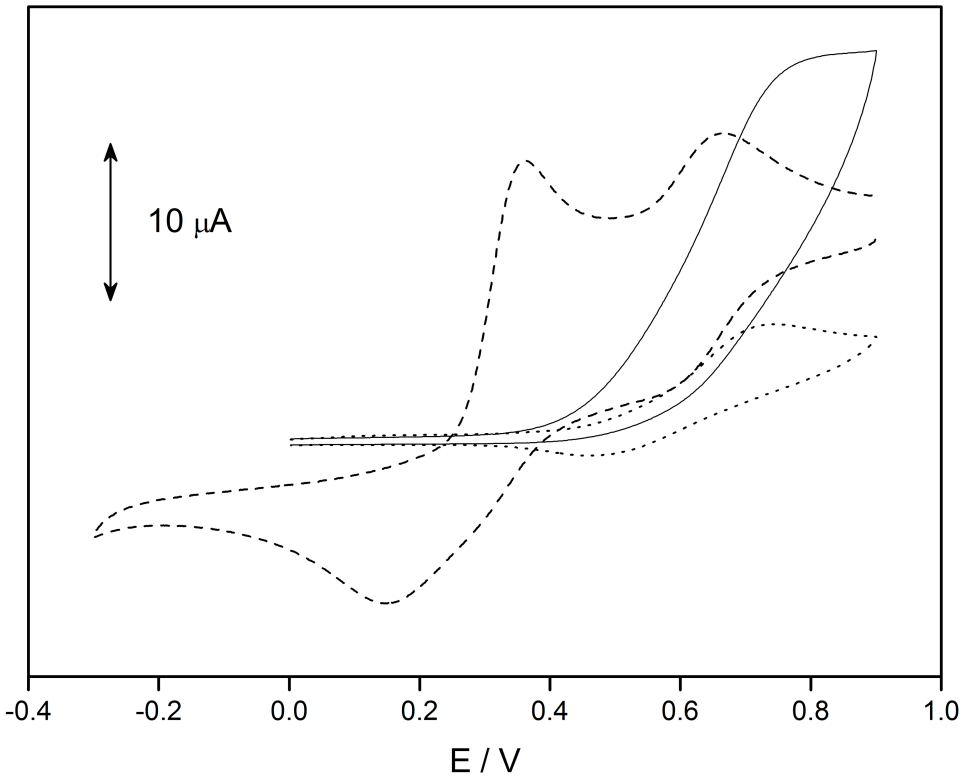

Fig. 6.3. Cyclic voltammograms of 1 mM solutions of $[Ni_6(cpss)_{12}]$ (−),$[Ni_6(cpss)_{12}]$ + $3I_2$ (---) and $[Ni_2(cpss)_2I_2]$ (· · ·) in CH_2Cl_2 containing 0.1M$(NBu_4)PF_6$. Scan rate 200 mV s^{-1}. Pt disc working, Pt wire counter electrodes used with a Ag/AgCl reference electrode.

6.2.5. Electronic Spectroscopic Studies of $[Ni_6(cpss)_{12}]$ in the Presence of H^+

To investigate the stability of the complex $[Ni_6L_{12}]$ in DMF, an electronic absorption spectrum was recorded; it displays three absorption bands at 29900 (LMCT), 24200 ($^1E''\leftarrow{}^1A_1'$) and 18200 ($^1E'\leftarrow{}^1A_1'$) cm^{-1} characteristic of a low-spin nickel(II) ion with a NiS_4 chromophore. The intensities of these absorptions remain unchanged in DMF solution for a prolonged period even after the addition of 12 equivalents of *p*-toluenesulfonic acid monohydrate ($TsOH{\cdot}H_2O$); they slowly decrease upon the addition of an excess of acid (>12 eq.) before they completely vanish only after several days (Fig. 6.4). Three new low-intensity peaks at 25600 (CT, obscuring $^3T_{1g}(P)\leftarrow{}^3A_{2g}$), 15000 ($^3T_{1g}\leftarrow{}^3A_{2g}$) and 13500 ($^1E_g\leftarrow{}^3A_{2g}$) cm^{-1} are observed after a week, associated with a change in the color of the solution from dark brown to light greenish-yellow. This change is ascribed to the disintegration of $[Ni_6L_{12}]$ upon protonation and by the excess acid present in the solution, resulting in the formation of solvent coordinated high-spin Ni(II) species. The same features are observed when dichloromethane is used as a solvent.

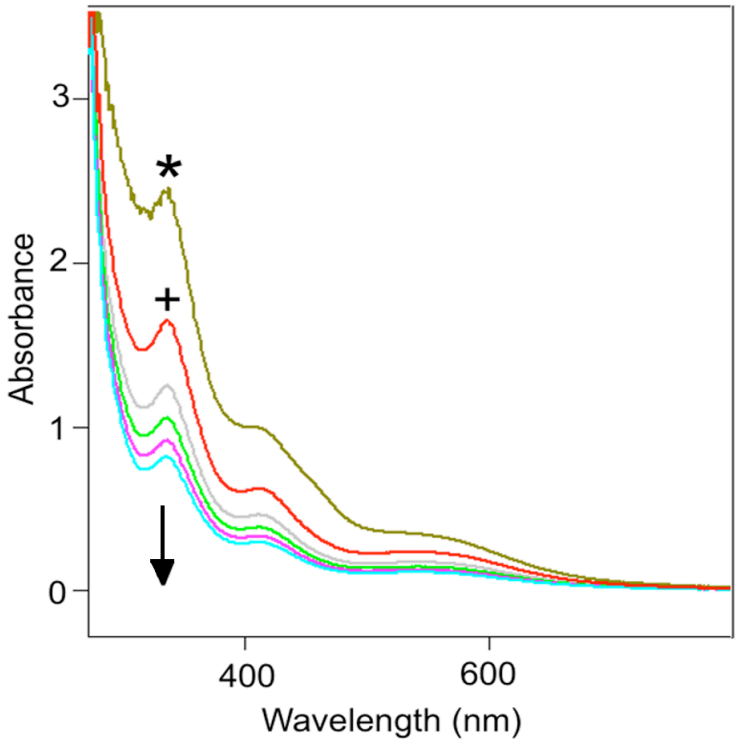

Fig. 6.4. Electronic absorption spectra of $[Ni_6(cpss)_{12}]$ (✱) and in the presence of a large excess of $[TsOH{\cdot}H_2O]$ (✚) in DMF; the remaining four spectra were recorded with 24 hour intervals between each.

6.2.6. ^{1}H NMR Spectroscopic Studies of $[Ni_6(cpss)_{12}]$

^{1}H NMR spectra of $[Ni_6(cpss)_{12}]$ have been recorded in DMF-d_7 solution to assess its stability in the presence of coordinating solvents (Fig. 6.5). Interestingly, the pattern of the ^{1}H NMR spectrum of $[Ni_6L_{12}]$ in DMF-d_7 completely resembles that recorded in CD_2Cl_2, ruling out a solvent interaction by coordination in the axial positions of Ni(II) ions in exchange for the axial coordination of the thioether donors. All the six axial positions present in the outer side of the Ni_6 ring of $[Ni_6(cpss)_{12}]$ are occupied by thioether sulfurs of the ligands alternatingly directed from above and below the Ni_6 ring (Fig. 6.5); six of the twelve ligands are monodentate and six ligands are bidentate as they use the thioether sulfur for the axial coordination.

The two doublets (7.49 and 7.37 ppm) and one singlet (7.32 ppm) of equal intensity in the aromatic region of the ^{1}H NMR spectra belong to the chelating ligands and the monodentate ligands, respectively. The aromatic protons of the monodentate ligands are showing a singlet, as the rings are free to rotate, while the aromatic protons of the chelating ligands show two doublets as a result of the restricted rotation. Furthermore, the room temperature ^{1}H NMR spectra of $[Ni_6(cpss)_{12}]$ in DMF-d_7 or in CD_2Cl_2 remain unchanged for several days, confirming the high stability of $[Ni_6(cpss)_{12}]$ in these solvents.

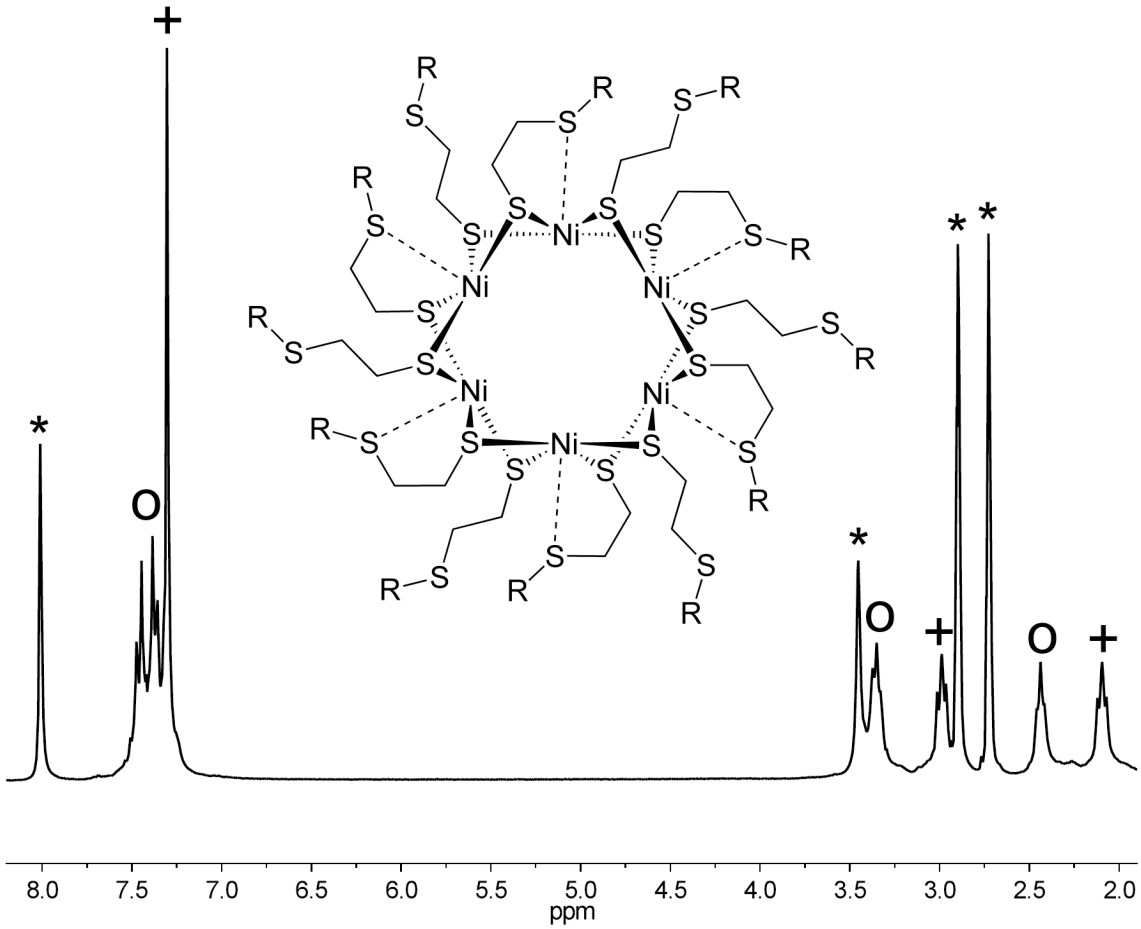

Fig. 6.5. ^{1}H NMR of [$Ni_6(cpss)_{12}$] in DMF-d_7 solution and the schematic diagram of the solution structure of [$Ni_6(cpss)_{12}$] (inset). R indicates the 4-chlorophenyl groups of the ligand; **+**, signals from monodentate ligands; **O**, signals from chelating ligands; ★, signals from residual protons of the solvent.

6.2.7. Protonation of [$Ni_6(cpss)_{12}$] as Studied by ^{1}H NMR Spectroscopy

The effect of the addition of protic acids to the CD_2Cl_2 solution of [$Ni_6(cpss)_{12}$] has been studied employing ^{1}H NMR spectroscopy. The gradual changes in the ^{1}H NMR spectrum upon the increasing addition of dichloroacetic acid to the solution of [$Ni_6(cpss)_{12}$] are shown in Fig. 6.6. Interestingly, the intensities of the signals of the monodentate ligands at 7.12, 2.87 and 2.01 ppm decrease in the initial stage of additions of the acid followed by the signals of the chelating ligands upon further additions. Simultaneously, a new set of signals grows at 7.30, 3.12 and 2.73 ppm, due to the protonation of the thioether sulfurs available from the twelve ligands. The same changes are observed when DMF-d_7 and *p*-toluenesulfonic acid monohydrate ($TsOH{\cdot}H_2O$) are used. Protonation of the cluster was further confirmed by the isotopic distribution patterns of the ESI-MS spectra: signals are found at m/z 467.75 and 468.11 for [$M+6H^+$]

(Fig. 6.7) and [M+6D⁺] (using DCl), respectively. The ^{1}H NMR spectrum of the protonated $[Ni_6L_{12}]$ in both CD_2Cl_2 (with dichloroacetic acid) and DMF-d_7 (with $TsOH{\cdot}H_2O$) remained unchanged even after two days, again confirming the high stability of the protonated $[Ni_6L_{12}]$ compound in solution. The signals slowly broaden upon the addition of a large excess of acid due to the formation of paramagnetic high-spin Ni(II) species, as also observed from the electronic absorption spectra.

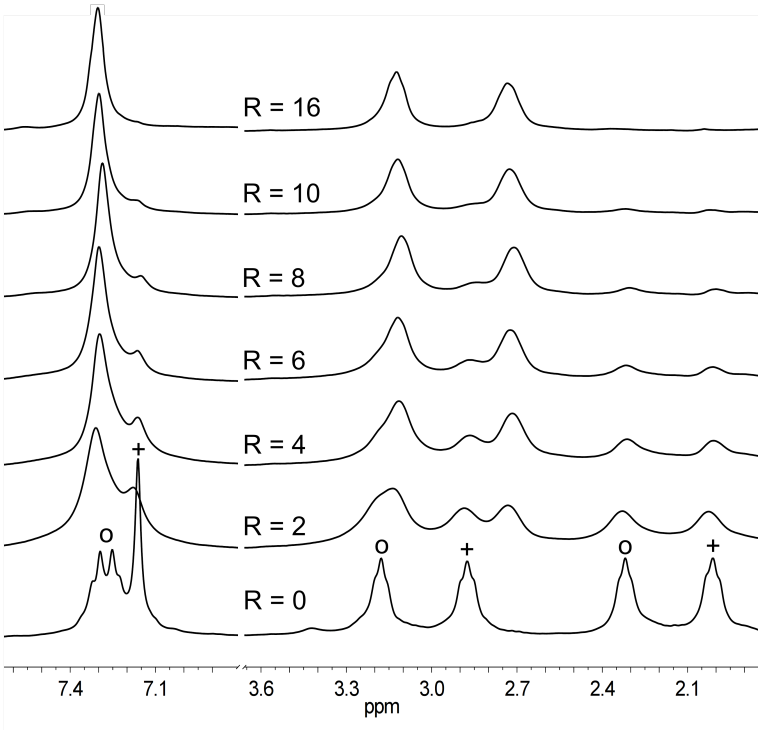

Fig. 6.6. ^{1}H NMR spectra of $[Ni_6(cpss)_{12}]$ in CD_2Cl_2 upon the addition of dichloroacetic acid in CD_2Cl_2 in various Ni to H^+ ratios. R = [acid]/[Ni]. **+**, signals from monodentate ligands; **O**, signals from chelating ligands.

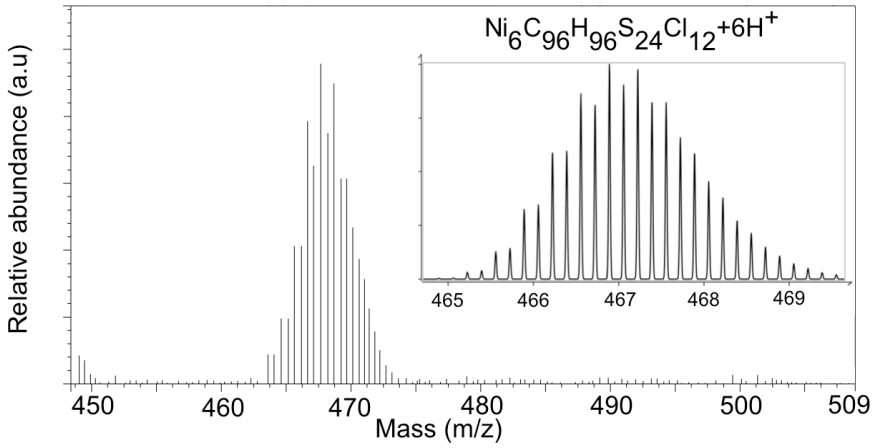

Fig. 6.7. Positive-ion ESI-MS spectrum of $[Ni_6(cpss)_{12}]$ in dichloromethane in the presence of trifluoromethanesulfonic acid; the isotopic distribution pattern simulated for $[Ni_6C_{96}H_{96}S_{24}Cl_{12}]+6H^+$ (inset).

6.2.8. Electrocatalytic H_2 Evolution by [$Ni_6(cpss)_{12}$]

Cyclic voltammograms of [$Ni_6(cpss)_{12}$] in the presence of up to twelve equivalents of protic acids, such as dichloroacetic acid and monochloroacetic acid were recorded in order to assess the electrochemical properties of the protonated [$Ni_6(cpss)_{12}$] cluster. The reduction peak of the [$Ni_6(cpss)_{12}$] wheel is slightly shifted towards more positive potential upon the protonation (–1.05 V) and a new reduction event appears around –1.5 V *vs*. Ag/AgCl; the current height of this new cathodic peak increases with increasing concentration of the acid (Fig. 6.8a).[29] This reduction is accompanied by the formation of bubbles on the surface of the electrode, confirming the production of dihydrogen gas by the electrocatalytic reduction of protons.[39,47] The positive shift in the reduction potential of the protonated [$Ni_6(cpss)_{12}$] complex is almost negligible, since the protonation of the thioether sulfur does not seem to affect the nickel(II) ion electronically, as indicated by the electronic absorption spectra. This rules out the direct protonation of the metal center prior to the reduction.[29] The definite peak-like shape of the catalytic reduction event is indicative of a diffusion-controlled electrocatalytic process and the catalytic reaction is rapid enough, so that the current is controlled by the diffusion of the substrate to the electrode surface.[39,47,48] The same experiment was carried out with monochloroacetic acid, in order to investigate the effect of the pK_a of the proton source. Despite the change in the pK_a, the reduction of the protonated [Ni_6L_{12}] complex occurs at the same potential as for dichloroacetic acid. However, the potential at which molecular hydrogen evolution occurs moved towards a slightly more negative potential of -1.6 V (Fig. 6.8b).[49]

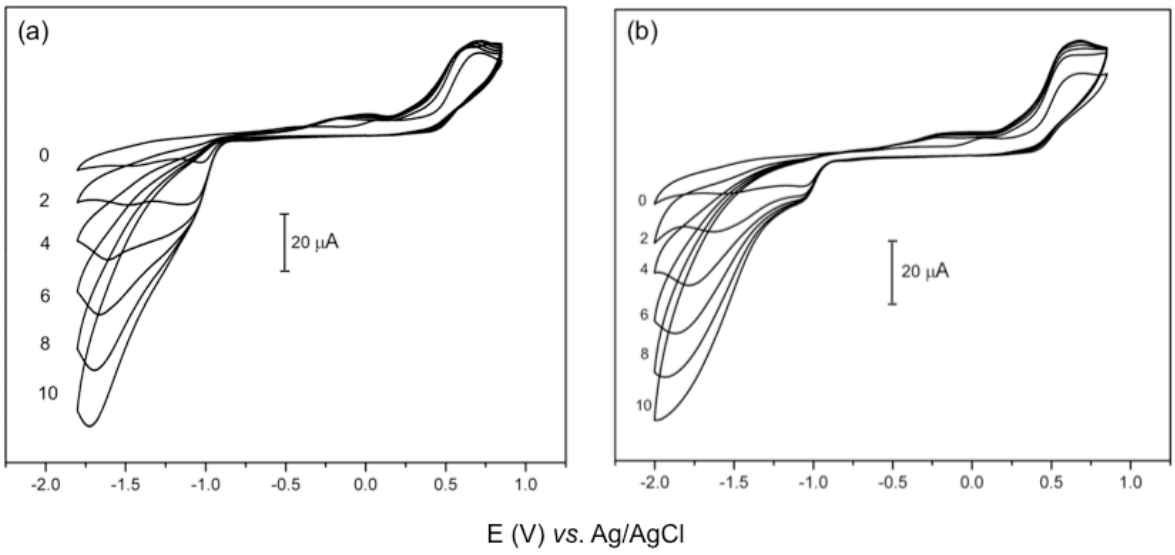

Fig. 6.8. Cyclic voltammograms of [$Ni_6(cpss)_{12}$] (0.5 mM in DMF + 0.1 M *n*-Bu_4NPF_6) in the absence (R = 0) and presence (R = [acid]/[Ni] = 2, 4, 6, 8, 10) of (a) dichloroacetic acid and (b) chloroacetic acid at a static glassy carbon working electrode with a Pt wire auxiliary electrode. Scan rate 200 mV/s.

6.2.9. Proposed Catalytic Mechanism

The axial coordination of two of the thioether sulfurs observed in the X-ray crystal structure, the protonation of the thioether sulfurs as observed with ^{1}H NMR spectroscopy and the electrochemical results described above, in combination, resulted in the following proposed catalytic cycle shown in Scheme 6.2.

Central in the proposed mechanism (Scheme 6.2) is the parent nickel(II) ion with a coordinated thioether sulfur. Protonation occurs at the thioether sulfurs as indicated by ^{1}H NMR spectroscopy and ESI-MS spectrometry. The protonated $[Ni_6(cpss)_{12}]$ complex is electrochemically reduced at –1.05 V. The second reduction observed at –1.5 V in the case of dichloroacetic acid and at –1.6 V in the case of chloroacetic acid must be accompanied by a second protonation step, thereby liberating molecular hydrogen and regenerating the catalyst. The absence of notable changes in the anodic wave in the cyclic voltammograms suggests that after the release of molecular hydrogen the oxidation part solely arises from the reformed $[Ni_6(cpss)_{12}]$ cluster. The participation of the reduced metal center in the dihydrogen evolution is further confirmed by the observation that dihydrogen evolution does not occur at around –1.5 V, when only the bidentate thioether-thiol ligand is used instead of $[Ni_6(cpss)_{12}]$.

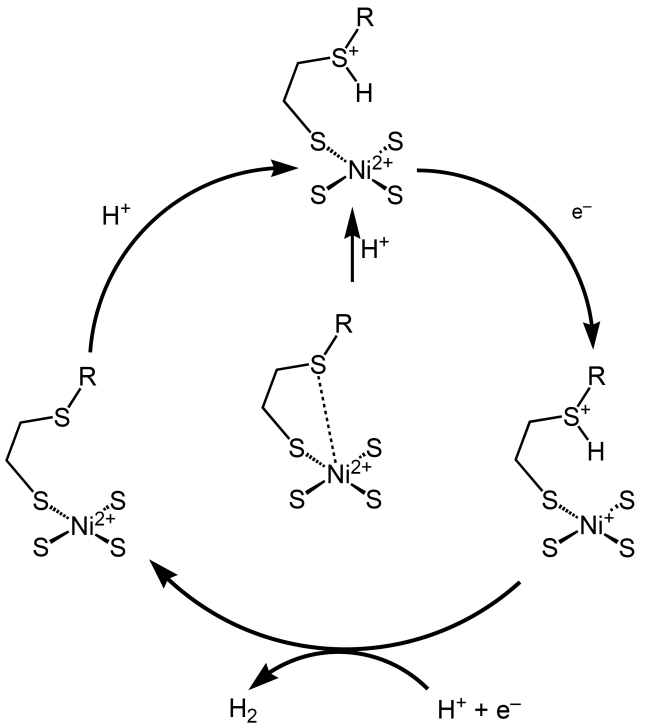

Scheme 6.2. Proposed mechanism of the catalytic cycle for the reduction of protons by $[Ni_6(cpss)_{12}]$ based on the protonation and electrochemical studies; the global charges are not indicated. Only one nickel center of the hexanuclear $[Ni_6(cpss)_{12}]$ complex is illustrated for the sake of clarity. R represents the 4-chlorophenyl group of the ligand.

6.2.10. Immobilization of [$Ni_6(cpss)_{12}$] on a Pyrolitic Graphite Electrode

In the view of possible application in proton exchange membranes[50,51] and in order to shed light on the mechanism of proton reduction, the [$Ni_6(cpss)_{12}$] cluster was immobilized on the surface of an edge plane pyrolitic graphite (EPPG) electrode using known immobilization techniques.[52] Furthermore, in this way the amount of catalyst used can be decreased and the reusability can be increased. Cyclic voltammograms of acetonitrile solutions of 0.1 M dichloroacetic were recorded using the EPPG before and after immobilization of the [$Ni_6(cpss)_{12}$] complex on the surface of the electrode.

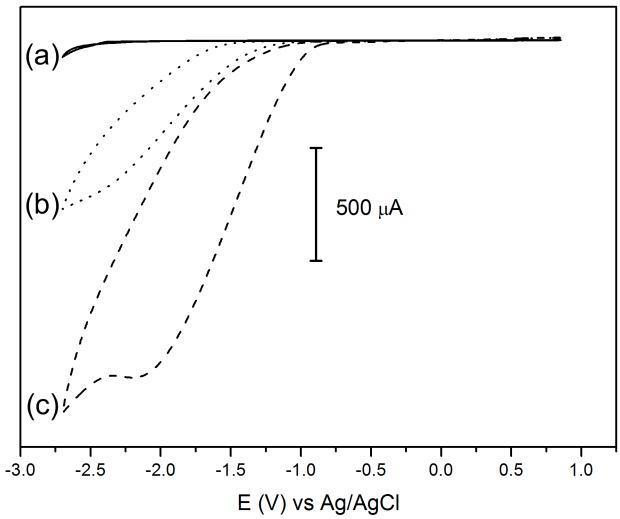

Fig. 6.9. Blank CV of acetonitrile (**a**); CV of a 0.1 M solution of dichloroacetic acid (**b**) containing 0.1 M *n*-Bu_4NPF_6 on a static edge plane pyrolitic graphite electrode; CV of 0.1 M solution of dichloroacetic acid (**c**) on a [$Ni_6(cpss)_{12}$]-immobilized static edge plane pyrolitic graphite electrode with a Pt wire auxiliary electrode (see experimental section for the details of immobilization). Scan rate 200 mV/s.

Reduction of dichloroacetic acid occurs around –2.35 V on the surface of the unmodified EPPG electrode, while the same event happens around –2.13 V after adsorption of the [$Ni_6(cpss)_{12}$] complex on the surface of the EPPG electrode (Fig. 6.1). The increase in the current height of the reduction peak and the shift in reduction potential to a more positive value by 220 mV clearly indicate the catalyzing ability of the [$Ni_6(cpss)_{12}$] cluster. The stability of the immobilized compound was checked with multiple runs of the cyclic voltammogram. After 30 scans the current height is unchanged, but the potential of the proton reduction has shifted towards slightly more negative potentials. Furthermore, a Tafel plot of the cyclic voltammogram of electrocatalytic proton reduction (log current density vs. potential), drawn between –1.2 and –1.8 V displays a slope of 75 mV/decade suggesting a Nernstian pre-equilibrium followed by a rate-determining chemical potential-independent step.[53] The deviation

from the value of 60 mV/decade may be due to a double-layer effect. Chemically this could imply that the proton binds from an equilibrium reaction and then some chemical rate-determining step, such as structural rearrangement or proton migration leads to H_2 or a precursor for H_2 formation; proton migration from the thioether sulfur to the reduced metal center may be involved in the catalytic cycle, as reported for the models of [FeFe] hydrogenases.[54-56]

6.3. Conclusions

In conclusion, the hexanuclear nickel(II)-thiolato cluster $[Ni_6(cpss)_{12}]$ has been synthesized, with NiS_4 square-planar and NiS_5 square-pyramidal units in the same molecule. The NiS_5 units resemble the Ni centre in [NiFe] hydrogenase.[44] The chemical oxidation of the $[Ni_6(cpss)_{12}]$ complex with iodine yields the dinuclear complex $[Ni_2(cpss)_2I_2]$ via an unstable intermediate as observed in the electrochemistry. The low-spin square-pyramidal nickel(II) center of the NiS_5 unit as observed from the X-ray crystal structure and from the ^1H NMR spectra of the $[Ni_6(cpss)_{12}]$ cluster, closely resembles the nickel(II) center of the [NiFe] hydrogenase in its Ni-R state.[27,57,58] The protonation of the low-spin hexanuclear nickel thiolate metallacrown $[Ni_6(cpss)_{12}]$, has been demonstrated using ^1H NMR spectroscopy and ESI-MS spectrometry. The protonated $[Ni_6(cpss)_{12}]$ complex is extremely stable, as studied by NMR and electronic spectroscopy. Furthermore, it was shown to be a functional mimic of hydrogenases, as it acts as an electrocatalyst with the evolution of dihydrogen in the presence of protons. Furthermore, the proposed catalytic cycle closely follows the route as proposed for the natural enzymatic system.[27,57,58] First, the $[Ni_6(cpss)_{12}]$ cluster is protonated and reduced (at –1.05 V vs Ag/AgCl); then, the second reduction step coupled with a protonation (at –1.5 or –1.6 V vs Ag/AgCl) induces the release of dihydrogen. In the proposed catalytic cycle of the hydrogenases, the Ni-SI state has a nickel(II) center and a protonated thiolate ligand, which undergoes reduction accompanied by proton abstraction to form the Ni-L state which contains a nickel(I) center.[27,57,58] Immobilization of the $[Ni_6(cpss)_{12}]$ cluster on an electrode surface further highlights its electrocatalytic ability.

6.4. Experimental Section

6.4.1. General

Synthesis of the ligand precursor TU-cpss is described in Chapter 2 along with the characterizations and other instrumental techniques.

6.4.2. Synthesis of $[Ni_6(cpss)_{12}]$

To a suspension of $[Ni(acac)_2]$ (0.51 g, 2 mmol) in 30 ml of toluene was added two equivalents of TU-cpss (1.13 g, 4 mmol). After the addition of two equivalents of NMe_4OH

(0.72 g, 4 mmol), the solution was refluxed for 2 h. The resulting brown solution was filtered and the solvent was evaporated under reduced pressure to give a dark brown oil. Ethanol (5 ml) was added to the dark brown oil yielding 0.63 g of a reddish–brown solid (yield 72%). Rectangular shaped tiny reddish–brown crystals suitable for X-ray diffraction were isolated from a solution of methanol and acetone (1 : 1) after standing for one day at room temperature. **^{1}H NMR**: δ_H [300.13 MHz, CD_2Cl_2, 298 K]) 7.31 (d, 2H, phenyl ring, chelate), 7.24 (d, 2H, phenyl ring, chelate), 7.12 (s, 4H, phenyl ring, monodentate), 3.18 (t, 2H, Ph-S-C*H*$_2$-CH$_2$-S-, chelate), 2.87 (t, 2H, Ph-S-C*H*$_2$-CH$_2$-S-, monodentate), 2.32 (t, 2H, Ph-S-CH$_2$-C*H*$_2$-S-, chelate), 2.01 (t, 2H, Ph-S-CH$_2$-C*H*$_2$-S-, monodentate). **^{13}C NMR:** δ_C [75.47 MHz, CD_2Cl_2, 298 K] 131.32 (Ph-C2, chelate), 130.64 (Ph-C2, monodentate), 129.58 (Ph-C3, chelate), 129.42 (Ph-C3, monodentate), 37.42 (Ph-S-*C*H$_2$-CH$_2$-S-, chelate), 34.59 (Ph-S-*C*H$_2$-CH$_2$-S-, monodentate), 32.25 (Ph-S-CH$_2$-*C*H$_2$-S-, chelate), 26.52 (Ph-S-CH$_2$-*C*H$_2$-S-, monodentate). **Elemental analysis (%):** calculated for $C_{96}H_{96}Cl_{12}Ni_6S_{24}$ (2796.95): C 41.23, H 3.46, S 27.51, found C 40.97, H 3.53, S 27.24.

6.4.3. Synthesis of [$Ni_2(cpss)_2I_2$]

To a solution of [$Ni_6(cpss)_{12}$] (0.28 g, 0.1 mmol) in 30 ml of dichloromethane was added a solution of three equivalents of iodine (0.076 g, 0.3 mmol) in 30 ml of dichloromethane and the reaction mixture was stirred for one hour at room temperature. After filtration of the white precipitate and evaporation of the solvent in open air for two days dark brown block-shaped crystals suitable for X-ray diffraction were isolated in 83% yield corresponding to [$Ni_2(cpss)_2I_2$]. **^{1}H NMR:** δ_H [300.13 MHz, CD_2Cl_2, 298 K] 7.30 (dd, 8H, phenyl ring), 3.19 (t, 4H, Ph-S-C*H*$_2$-CH$_2$-S-), 2.83 (t, 4H, Ph-S-CH$_2$-C*H*$_2$-S-). **^{13}C NMR:** δ_C [75.47 MHz, CD_2Cl_2, 298 K] 131.26 (Ph-C2), 129.32 (Ph-C3), 37.23 (Ph-S-*C*H$_2$-CH$_2$-S-), 32.03 (Ph-S-CH$_2$-*C*H$_2$-S-). **Elemental analysis (%):** calculated for $C_{16}H_{16}Cl_2I_2Ni_2S_4$ (778.65): C 24.68, H 2.07, S 16.47, found C 24.53, H 1.98, S 16.29.

6.4.4. Crystallographic data for [$Ni_6(cpss)_{12}$]

Reflections were measured on a Nonius Kappa CCD diffractometer with rotating anode (graphite monochromator, λ = 0.71073 Å) at a temperature of 150 K. The structures were solved with automated Patterson methods using the program DIRDIF[59] and refined with SHELXL-97[60] against F^2 of all reflections. Non-hydrogen atoms were refined with anisotropic displacement parameters. Hydrogen atoms were refined with a riding model. Geometry calculations and checking for higher symmetry was performed with the PLATON program.[61]

$C_{96}H_{96}Cl_{12}Ni_6S_{24}$, Fw = 2796.95, 0.28 × 0.04 × 0.02 mm^3, triclinic, P-1 (no. 2), a = 11.8667(12), b = 13.9186(12), c = 18.843(2) Å, α = 75.996(11), β = 76.080(11), γ =

74.991(13)°, V = 2863.7(5) Å^3, Z = 1, D_x = 1.622 g cm^{-3}, μ = 1.73 mm^{-1}. 55 395 Reflections were measured up to a resolution of (sin $\theta/\lambda)_{max}$ = 0.60 Å^{-1}. An absorption correction based on multiple measured reflections was applied (0.64–0.0.97 correction range). 10 355 Reflections were unique (R_{int} = 0.1398), of which 6121 were observed [$I > 2\sigma(I)$]. 622 Parameters were refined with no restraints. $R1/wR2$ [$I > 2\sigma(I)$]: 0.0596/0.0863. $R1/wR2$ [all refl.]: 0.1311/0.1048. S = 1.049. Residual electron density between −0.47 and 0.54 eÅ^{-3}.

6.4.5. Crystallographic data for $[Ni_2(cpss)_2I_2]$

$C_{16}H_{16}Cl_2I_2Ni_2S_4$, Fw = 778.65, 0.36 × 0.21 × 0.03 mm^3, monoclinic, $C2/c$ (no. 15), a = 16.4582(5), b = 15.0185(6), c = 9.8037(2) A°, β = 110.134(2)◦, V = 2275.16(13) Å^3, Z = 4, D_x = 2.273 g cm^{-3}, μ = 4.97 mm^{-1}. 20 584 Reflections were measured up to a resolution of (sin θ/λ)max = 0.65A° Å^{-1}. An absorption correction based on multiple measured reflections was applied (0.33–0.0.86 correction range). 2622 Reflections were unique (R_{int} = 0.0311), of which 2179 were observed [$I > 2\sigma(I)$]. 118 Parameters were refined with no restraints. $R1/wR2$ [$I > 2\sigma(I)$]: 0.0203/0.0387. $R1/wR2$ [all refl.]: 0.0319/0.0413. S = 1.056. Residual electron density between −0.42 and 0.37 eÅ^{-3}.

6.5. References

1. V. Artero and M. Fontecave, *Coord. Chem. Rev.*, 2005, **249**, 1518-1535.
2. S. P. Best, *Coord. Chem. Rev.*, 2005, **249**, 1536-1554.
3. C. Zhang, S. Takada, M. Kolzer, T. Matsumoto and K. Tatsumi, *Angew. Chem.-Int. Edit. Engl.*, 2006, **45**, 3768-3772.
4. E. Bouwman and J. Reedijk, *Coord. Chem. Rev.*, 2005, **249**, 1555-1581.
5. P. M. Vignais, *Coord. Chem. Rev.*, 2005, **249**, 1677-1690.
6. R. Cammack, R. Frey and R. Robson, *Hydrogen as a Fuel. Learning from Nature*, Taylor & Francis, London, 2001.
7. M. Murugesu, F. Wernsdorfer, K. A. Abboud and G. Christou, *Angew. Chem.-Int. Edit.*, 2005, **44**, 892-896.
8. S. Piligkos, G. Rajaraman, M. Soler, N. Kirchner, J. van Slageren, R. Bircher, S. Parsons, H. U. Gudel, J. Kortus, W. Wernsdorfer, G. Christou and E. K. Brechin, *J. Am. Chem. Soc.*, 2005, **127**, 5572-5580.
9. A. J. Tasiopoulos, A. Vinslava, W. Wernsdorfer, K. A. Abboud and G. Christou, *Angew. Chem.-Int. Edit.*, 2004, **43**, 2117-2121.
10. C. M. Zaleski, E. C. Depperman, J. W. Kampf, M. L. Kirk and V. L. Pecoraro, *Angew. Chem.-Int. Edit.*, 2004, **43**, 3912-3914.
11. F. K. Larsen, J. Overgaard, S. Parsons, E. Rentschler, A. A. Smith, G. A. Timco and R. E. P. Winpenny, *Angew. Chem.-Int. Edit.*, 2003, **42**, 5978-5981.
12. L. E. Jones, A. Batsanov, E. K. Brechin, D. Collison, M. Helliwell, T. Mallah, E. J. L. McInnes and S. Piligkos, *Angew. Chem.-Int. Edit.*, 2002, **41**, 4318-4321.
13. A. L. Dearden, S. Parsons and R. E. P. Winpenny, *Angew. Chem.-Int. Edit.*, 2001, **40**, 151-154.
14. S. X. Liu, S. Lin, B. Z. Lin, C. C. Lin and J. Q. Huang, *Angew. Chem.-Int. Edit.*, 2001, **40**, 1084-+.
15. S. P. Watton, P. Fuhrmann, L. E. Pence, A. Caneschi, A. Cornia, G. L. Abbati and S. J. Lippard, *Angew. Chem.-Int. Edit.*, 1997, **36**, 2774-2776.
16. J. Sletten and J. A. Kovacs, *Acta Chem. Scand.*, 1994, **48**, 929-932.

17. M. Capdevila, P. Gonzalezduarte, J. Sola, C. Focesfoces, F. H. Cano and M. Martinezripoll, *Polyhedron*, 1989, **8**, 1253-1259.
18. W. Gaete, J. Ros, X. Solans, M. Fontaltaba and J. L. Brianso, *Inorg. Chem.*, 1984, **23**, 39-43.
19. P. Woodward, L. F. Dahl, E. W. Abel and B. C. Crosse, *J. Am. Chem. Soc.*, 1965, **87**, 5251-&.
20. Z. Yu, M. Wang, P. Li, W. B. Dong, F. J. Wang and L. C. Sun, *Dalton Trans.*, 2008, 2400-2406.
21. B. Keita, S. Floquet, J. F. Lemonnier, E. Cadot, A. Kachmar, M. Benard, M. M. Rohmer and L. Nadjo, *J. Phys. Chem. C*, 2008, **112**, 1109-1114.
22. L. C. Song, Z. Y. Yang, Y. J. Hua, H. T. Wang, Y. Liu and Q. M. Hu, *Organometallics*, 2007, **26**, 2106-2110.
23. Y. Oudart, V. Artero, J. Pecaut, C. Lebrun and M. Fontecave, *Eur. J. Inorg. Chem.*, 2007, 2613-2626.
24. X. Hu, B. S. Brunschwig and J. C. Peters, *J. Am. Chem. Soc.*, 2007, **129**, 8988-8998.
25. G. A. N. Felton, A. K. Vannucci, J. Z. Chen, L. T. Lockett, N. Okumura, B. J. Petro, U. I. Zakai, D. H. Evans, R. S. Glass and D. L. Lichtenberger, *J. Am. Chem. Soc.*, 2007, **129**, 12521-12530.
26. A. M. Appel, D. L. DuBois and M. R. DuBois, *J. Am. Chem. Soc.*, 2005, **127**, 12717-12726.
27. J. C. Fontecilla-Camps, A. Volbeda, C. Cavazza and Y. Nicolet, *Chem. Rev.*, 2007, **107**, 4273-4303.
28. C. Tard, X. M. Liu, S. K. Ibrahim, M. Bruschi, L. De Gioia, S. C. Davies, X. Yang, L. S. Wang, G. Sawers and C. J. Pickett, *Nature*, 2005, **433**, 610-613.
29. S. Ott, M. Kritikos, B. Åkermark, L. C. Sun and R. Lomoth, *Angew. Chem.-Int. Edit.*, 2004, **43**, 1006-1009.
30. A. Volbeda, M. H. Charon, C. Piras, E. C. Hatchikian, M. Frey and J. C. Fontecilla-Camps, *Nature*, 1995, **373**, 580-587.
31. J. A. W. Verhagen, D. D. Ellis, M. Lutz, A. L. Spek and E. Bouwman, *J. Chem. Soc.-Dalton Trans.*, 2002, 1275-1280.
32. H. J. Kruger, G. Peng and R. H. Holm, *Inorg. Chem.*, 1991, **30**, 734-742.
33. Y. Oudart, V. Artero, J. Pecaut and M. Fontecave, *Inorg. Chem.*, 2006, **45**, 4334-4336.
34. S. Canaguier, V. Artero and M. Fontecave, *Dalton Trans.*, 2008, 315-325.
35. Y. Ohki, K. Yasumura, K. Kuge, S. Tanino, M. Ando, Z. Li and K. Tatsumi, *Proc. Natl. Acad. Sci. U. S. A.*, 2008, **105**, 7652-7657.
36. Z. L. Li, Y. Ohki and K. Tatsumi, *J. Am. Chem. Soc.*, 2005, **127**, 8950-8951.
37. X. Hu, B. M. Cossairt, B. S. Brunschwig, N. S. Lewis and J. C. Peters, *Chem. Commun.*, 2005, 4723-4725.
38. O. Pantani, E. Anxolabéhére-Mallart, A. Aukauloo and P. Millet, *Electrochem. Commun.*, 2007, **9**, 54-58.
39. I. Bhugun, D. Lexa and J. M. Saveant, *J. Am. Chem. Soc.*, 1996, **118**, 3982-3983.
40. J. P. Collman, Y. Y. Ha, P. S. Wagenknecht, M. A. Lopez and R. Guilard, *J. Am. Chem. Soc.*, 1993, **115**, 9080-9088.
41. V. Artero and M. Fontecave, *C. R. Chim.*, 2008, **11**, 926-931.
42. O. Pantani, S. Naskar, R. Guillot, P. Millet, E. Anxolabéhére-Mallart and A. Aukauloo, *Angew. Chem., Int. Ed. Engl.*, 2008, **47**, 9948-9950.
43. A. W. Addison, T. N. Rao, J. Reedijk, J. van Rijn and G. C. Verschoor, *J. Chem. Soc.-Dalton Trans.*, 1984, 1349-1356.
44. A. Volbeda, E. Garcia, C. Piras, A. L. deLacey, V. M. Fernandez, E. C. Hatchikian, M. Frey and J. C. FontecillaCamps, *J. Am. Chem. Soc.*, 1996, **118**, 12989-12996.
45. T. J. Mooibroek and P. Gamez, *Inorg. Chim. Acta*, 2007, **360**, 381-404.
46. T. J. Mooibroek, S. J. Teat, C. Massera, P. Gamez and J. Reedijk, *Cryst. Growth Des.*, 2006, **6**, 1569-1574.
47. C. P. Andrieux, C. Blocman, J. M. Dumas-Bouchiat, F. M' Halla and J. M. Savéant, *J. Electroanal. Chem.*, 1980, **113**, 19-40.
48. J. M. Savéant and K. B. Su, *J. Electroanal. Chem.*, 1984, **171**, 341-349.
49. G. A. N. Felton, R. S. Glass, D. L. Lichtenberger and D. H. Evans, *Inorg. Chem.*, 2006, **45**, 9181-9184.
50. P. Millet, F. Andolfatto and R. Durand, *Int. J. Hydrog. Energy*, 1996, **21**, 87-93.

51. P. Millet, T. Alleau and R. Durand, *J. Appl. Electrochem.*, 1993, **23**, 322-331.
52. M. T. De Groot and M. T. M. Koper, *Phys. Chem. Chem. Phys.*, 2008, **10**, 1023-1031.
53. A. J. Bard and L. R. Faulkner, *Electrochemical Methods: Fundamentals and Applications*, John Wiley & Sons, Inc., New York, 2001.
54. C. Greco, M. Bruschi, L. De Gioia and U. Ryde, *Inorg. Chem.*, 2007, **46**, 5911-5921.
55. C. Greco, G. Zampella, L. Bertini, M. Bruschi, P. Fantucci and L. De Gioia, *Inorg. Chem.*, 2007, **46**, 108-116.
56. J.-F. Capon, F. Gloaguen, F. Y. PÈtillon, P. Schollhammer and J. Talarmin, *Coord. Chem. Rev.*, 2009, **253**, 1476-1494.
57. A. L. DeLacey, V. M. Fernandez, M. Rousset and R. Cammack, *Chem. Rev.*, 2007, **107**, 4304-4330.
58. A. Pardo, A. L. De Lacey, V. M. Fernandez, H. J. Fan, Y. B. Fan and M. B. Hall, *J. Biol. Inorg. Chem.*, 2006, **11**, 286-306.
59. P. T. Beurskens, G. Admiraal, G. Beurskens, W. P. Bosman, S. Garcia-Granda, R. O. Gould, J. M. M. Smits and C. Smykalla, University of Nijmegen, The Netherlands, **1999**.
60. G. M. Sheldrick, University of Göttingen, Germany, **1997**.
61. A. L. Spek, *J. Appl. Crystallogr.*, 2003, **36**, 7-13.